

Reversal of the surface charge of a mineral powder: application to electrophoretic deposition of silica for anticorrosion coatings

B. CABOT, A. FOISSY

*Laboratoire d'Electrochimie et des Systèmes Microdispersés, Route de Gray,
25030 Besançon Cedex, France*

E-mail: benjanin.cabot@univ-fonte.fr

Electrophoretic deposition is used to produce a silica layer on zinc-coated steel and chromated zinc-coated steel. This type of coating is commonly employed in car industries to protect steel against corrosion. Because of the presence of zinc and chromated layers on the substrate, the polarization must be cathodic to avoid oxidation. Reversal of the silica surface charge is obtained using different methods, such as cation adsorption, cationic polymer (polyvinylimidazole) adsorption or oxide (cerium oxide) adsorption. The production of deposits using cations is quite difficult because it is necessary to add a high concentration of salt to reverse the silica charge, provoking high conductivity and gas release at the cathode. With polyvinylimidazole, the instability of the polymer is also a restrictive factor for the application of electrophoresis. The most promising results are obtained with ceriacovered silica. In fact the system is stable under the electric field and allows homogeneous coatings to be produced. The polarization resistance measurements indicate the good protective effect compared with the untreated substrate. © 1998 Kluwer Academic publishers

1. Introduction

Silica can be deposited onto surfaces to increase the protection of metallic substrates against corrosion. The deposition is possible using different techniques such as dip coating or electrophoresis. In this paper we shall develop the coating by electrophoretic deposition (EPD). A complete state of the art of this method has been well depicted in the literature by Sarkar and Nicholson [1].

EPD has been used in the past to coat metal substrates with organic materials, especially in the car industry, to make a thermal barrier and to shape ceramic membranes [2, 3]. Very recently this technique has gained some renewed interest for the fabrication of microlaminated materials [4] and the deposition of textured superconducting thick films [5]. Advantages that can be drawn from the above chemical deposition techniques are low cost and thickness uniformity, even in hidden parts of complex shapes. In the case of electrophoretic deposition, an interesting opportunity is the control of the thickness and the deposition rate via the applied potential.

When the deposited layer is a composite material (a mixture of oxide + inorganic or organic additives), wet chemistry may generate a homogeneous and intimate distribution of the components. This requires the preparation of an adequate sol or a colloidal dispersion where the particles have been formerly co-aggregated or where the additives have been adsorbed onto the particles surface. The deposition of ceramic films from solid-liquid dispersions requires expertise

in the control of the dispersion properties. Surface reactivities, additive adsorption, surface charge density, particle aggregation and particle adhesion are some of the properties determining those of the film that the sol will generate.

Our experiments are made on substrates covered with an electrolytic zinc layer and a chromate conversion coating; therefore the polarization had to be cathodic (negatively charged substrate) in order to avoid dissolution of chromate layer and oxidation of the zinc coating.

Because the silica charge is negative above pH 2, it is first necessary to reverse it before carrying out EPD. We then present the different methods which allow this surface modification. The first method for making silica positive is to adsorb some metallic ions on the surface. It is admitted that the mechanism of cation adsorption is associated with proton release from surface hydroxyl groups [6]. Supporting this hypothesis, Kozawa [7] has shown that adsorption of zinc ions on silica increases with increasing pH of the solution up to 7 and then decreases. He proposed a surface complex mechanism for metal ion adsorption, including the fact that the silica surface is acting as bidentate ligand for the zinc cation.

It is also possible to reverse the charge with cationic polymer or surfactants. The effect of the particle size of colloidal silica on the amount of cationic polymer required for flocculation and charge reversal was investigated by Iler [8]. Bohmer *et al.* [9] also studied the adsorption of a cationic polyvinylimidazole (PVI)

on silica and Y_2O_3 ; they noticed the influence of the polymer charge on the amount adsorbed and on the chain configuration on the surface.

Adsorption of positive mineral oxide in the pH range investigated can also be used to produce positive silica particles. Cerium oxide seems to be appropriate because the particles have a positive surface charge up to pH 8.5; moreover this oxide is known to have some anticorrosion properties.

2. Materials and methods

2.1. Materials

2.1.1. Mineral powders

The silica sols employed in this work are made in the laboratory by precipitation of sodium silicate solutions in acidic medium. This method presents the opportunity to control perfectly the surface properties of the particles, their size and the sols monodispersity. The particle diameter is 20 nm, with a Brunauer–Emmett–Teller (BET) nitrogen surface area of about $145 \text{ m}^2 \text{ g}^{-1}$.

Nanometric ceria particles were provided by Rhône-Poulenc (Aubervilliers, France). They were obtained through the precipitation of $Ce^{4+}(NO_3^-)_4$ salt at very low pH. In water it redisperses spontaneously to form a stable colloidal sol in the pH range 0.5–2.5 [10]. This sol is transparent with a clear yellow colour, the particles diameter is 5 nm, with a BET nitrogen surface area of $135 \text{ m}^2 \text{ g}^{-1}$.

2.1.2. Polymers

Different types of PVI were obtained from Laboratoire Matériaux et Procédés Membranaires, Université des Sciences et Techniques du Languedoc, Montpellier, France. The synthesis of PVI is made in methanol for low molecular weights or benzene for higher molecular weights [11]. The formula is given in Fig. 1. Protometric measurements of PVI solutions indicate that molecules are strongly charged at pH 4; 70% of amine groups are protonated. Another way to make positive PVI molecules, independently of pH, is grafting methylated groups on amine functions to generate quaternary ammonium groups (Fig. 1). The quaternization ratio, q , varies in the range 0–52%.

2.1.3. Latex solutions

Latex solutions (from BASF) are employed after being washed using dialysis membranes. This procedure is

necessary to remove the synthesis residues which are present both on the particle surface and in the solution.

Other chemicals (poly(vinyl alcohol) (PVA) poly(ethylene glycol) (PEG) etc. used in this study were reagent analytical grade; water was purified by the Milli-Q water purification system.

2.2. Methods

Several techniques can be used to coat metals with an inorganic layer: sputtering, chemical vapour deposition, plasma spraying, immersions in a dispersion of particles in a liquid medium, sol–gel transition techniques, electrophoresis or any combination of these last procedures [12–14].

In this paper, we present electrophoretically made coatings on zinc-coated steel and chromated zinc-coated steel. EPD involves the flux of charged particles in a suspension under the influence of an electric field and their deposition on one of the electrodes. EPD can be compared with sedimentation [15, 16] because the first function of the applied electric field in EPD is to move particles towards one of the electrodes, similarly to the action of gravity in sedimentation phenomena. The choice of the electric field, i.e., the electrode polarization, results from a compromise between a sufficiently high deposition rate and the electrical charge transfer kinetics. It is worth noting that the deposition of particles at the electrode requires that they lose their electrical charge. The deposition yield depends therefore on the particles' ability to neutralize the surface charge at the electrode (e.g. adsorbed protons reduce to hydrogen molecules).

Deposits are made using a two-electrode cell and a power supply allowing the application of a constant potential.

2.2.1. Electrophoretic mobility measurements

These were made in order to evaluate the influence of adsorption on the net particle charge. Measurements were made using a zeta-sizer 2C apparatus (Malvern). The procedure was the following: silica particles were equilibrated for 1 day in a solution of the surface acting species (Zn^{2+} or La^{3+} , PVI polymers or CeO_2 colloids). Silica was then centrifuged out of the suspension and a small amount was reintroduced in the solution in order to proceed with the electrophoretic

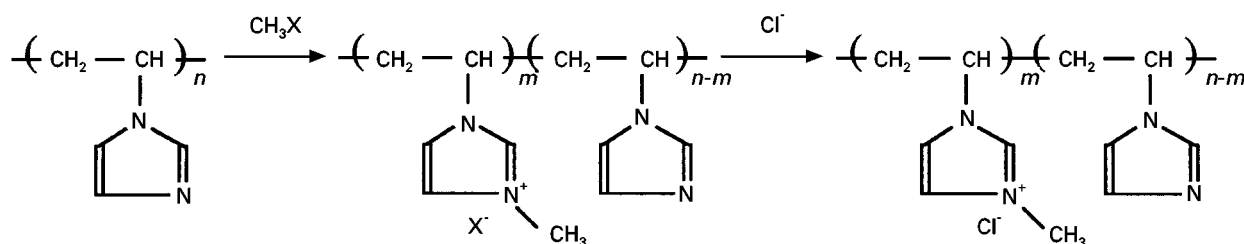


Figure 1 Structural formula of PVI and quaternized PVI.

measurement in a sufficiently diluted suspension. The later procedure is required to avoid desorption phenomena that would possibly occur if the samples were simply diluted by water addition. The zeta potential, ζ , has been calculated from the electrophoretic mobility, μ , using the Smoluchowski equation

$$\zeta = \frac{\eta}{\varepsilon} \mu \quad (1)$$

η is the viscosity and $\varepsilon (= \varepsilon_0 \varepsilon_r)$ is the permittivity of the medium.

2.2.2. Deposited layer characterizations

The morphological aspect of the coatings is examined by scanning electron microscopy (SEM) and X-ray photoelectron spectroscopy (XPS) analysis.

The electrochemical behaviour of the silica layer is studied by polarization resistance, R_p measurements. This method involves a potential scanning of small amplitude (about 10 mV) around the rest potential of the sample [17]. Knowing the electric current, the polarization resistance can then be calculated as

$$R_p = \frac{dE}{di} (\Omega \text{ cm}^{-2}) \quad (2)$$

The polarization resistance is defined as the polarization curve slope at the corrosion potential. It is connected to the corrosion current through the Stern–Geary [18] relationship

$$R_p = \frac{\beta_a \beta_c}{2.3 i_{\text{corr}} (\beta_a \beta_c)} \quad (3)$$

where β_a and β_c are the anodic and the cathodic slopes, respectively, of the Tafel curves. So it is clear that knowledge of the polarization resistance is a way to evaluate the corrosion current through a layer, and then to discriminate between several coatings on the basis of their anticorrosive properties. R_p measurements were made using a 3% NaCl solution (0.5 mol l^{-1}) and a three-electrode electrochemical cell. The working electrode has a 2 cm^2 surface area, the counterelectrode was a platinum wire and the reference was a KCl saturated calomel electrode.

3. Results and discussion

3.1. Silica charge control using cation adsorption

The first procedure employed to reverse the surface charge of silica particles is adsorption of multivalent ions. In fact, silanol groups on the silica surface start being ionized as SiO^- above pH 2, which induces a favourable electrostatic force for the adsorption of dissolved cations. The adsorption mechanism of hydrolysed metallic ions has received much attention [19]. A thermodynamic model of the system was proposed. James and Healy [20] have pointed out that the coulombic and chemical free energy changes, favourable to adsorption, balance the unfavourable desolvation required for a close contact of the cation with the particle surface. Considering adsorption of

divalent ions such as Ca^{2+} and Zn^{2+} , we can, however, imagine two types of binding. In the first case, the cation reacts with one silanol group, giving the complex a positive charge and allowing cathodic deposition. The second case does not show any charge reversal, indicating that a bidentate binding probably takes place between surface silanols and the cations.

The electrophoretic mobility curves of silica with zinc and lanthanum (Fig. 2) tend to indicate that the second case applies. These curves are obtained with a suspension of 1 wt% silica with increasing concentration of zinc sulphate or lanthanum chloride. Another problem occurs at high salt concentrations; the ionic strength is too high and electrolysis interferes with particle deposition.

There is, however, a way to make cathodic deposits with zinc-treated silica. The adsorption of a non ionic polymer, such as PEG ($M_w = 35000 \text{ g mol}^{-1}$), allows the silica particles to be made positive. This charge derives from the binding of zinc ions with the water-solvated oxygen atoms on PEG, which further adsorbs quite strongly on the silica surface, giving a net positive charge to the particles. The most significant problem here is to avoid precipitation of zinc hydroxides, by maintaining the pH below 7.

The cathodic polarization was done in a bath containing 1 wt% silica, 30 wt% PEG– SiO_2 and ZnSO_4 (0.05 mol l^{-1}). The electric field applied between the working electrode and the counterelectrode is set at -1.5 V cm^{-1} . A higher value would generate some hydrogen bubbling, which is a major drawback in the deposition process. The mass gain as a function of time (Fig. 3) tends to indicate that a plateau is reached after a polarization time of about 60 min. At this point the deposited layer on the electrode probably functions as an insulator, decreasing the electric field and preventing further deposition. We note that zinc-doped silica particles behave well in cataphoretic deposition. The synthesis consists in replacing some silicon by Zn ions on the superficial layers at the end of the particle synthesis. As with other cations the reactivity of the silanol groups is altered significantly by adjacent foreign ions [21].

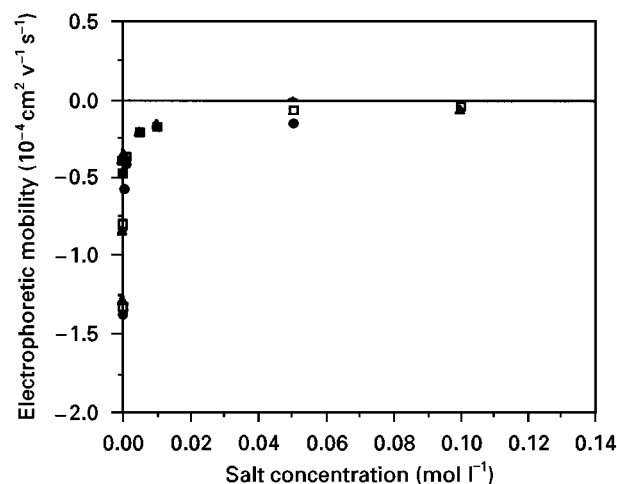


Figure 2 Influence of salt concentration on the electrophoretic mobility of silica (●), ZnSO_4 ; (□), LaCl_3 .

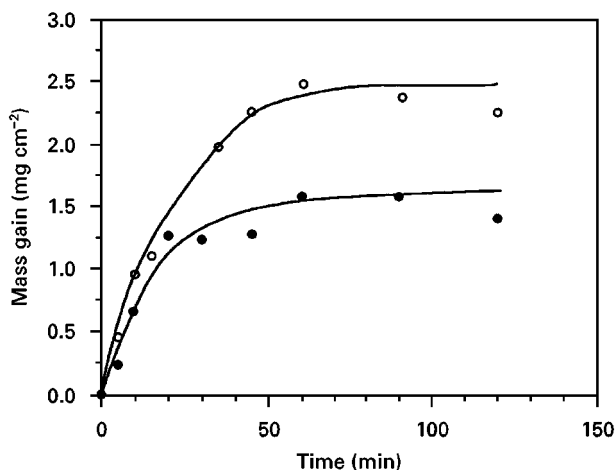


Figure 3 Cathodic deposition of silica: influence of surface treatment. (●), undoped silica; (○), doped silica.

The SEM analysis allows underline the following points to be emphasised. After a 5 min deposition, the layer structure looks like needles with a high amount of zinc (of thickness about 2 μm). The silica (8 wt% of the deposit) is distributed as agglomerates and dispersed on the needles (Fig. 4). At longer deposition times the structure of the layer changes. It starts to form nodules looking like cauliflower-shaped crystals, combined with the needles (Fig. 5). The silica still concentrates on the outer boundary. After 45 min, the morphological aspect of the layer is quite different (Fig. 6); needles have almost disappeared, leaving essentially nodules on the surface. The XPS analysis reveals that the average silica-zinc ratio decreases with time (there is only 5.5 wt% silica lying on the surface). The thickness is 3 μm ; it is non compact, with many interstices. The profile view of this layer (Fig. 7) indicates that it is not homogeneous; XPS analysis indicates an underlayer rich in zinc, but it cannot be assimilated to electrolytic zinc because it is less dense. The superficial part is richer in silica. This heterogeneity may be explained by a diffusion of zinc ions through the film, then being reduced as metallic zinc when arriving on the cathode. For a much longer deposition time (90 min), the needles have completely disappeared. The silica to Zn ratio is low (about 2 wt% silica in the outer layer). These results are in good agreement with those of Takahashi *et al.* [22] who studied the electrodeposition of zinc-iron and zinc-chromium composites with SiO_2 colloids. The amount of oxide in the layer varied from 8 to 10%, and they also noticed that silica was incorporated in the layer as aggregates. The aggregates, in the case of zinc-iron alloys, were deposited at the cathode because of the positive charge due to the iron adsorption onto the silica surface. In the case of zinc-chromium alloys, silica catalysed the electrolytic Cr codeposition.

3.2. Silica charge control using cationic polymer adsorption

Cationic polymers are strongly adsorbed from water on the silica surface over the whole pH range if no

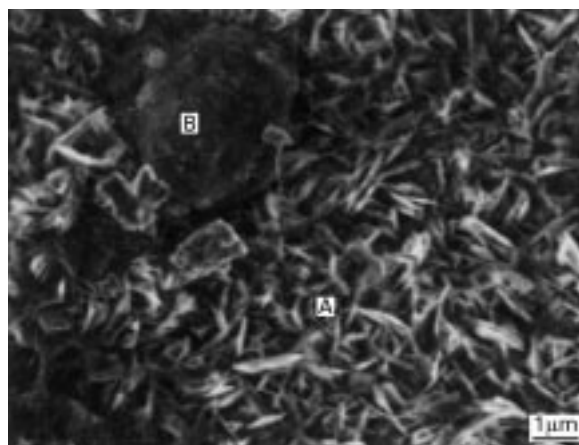


Figure 4 Details of silica-zinc deposit after 5 min polarization. A, needles of zinc; B, amorphous silica.

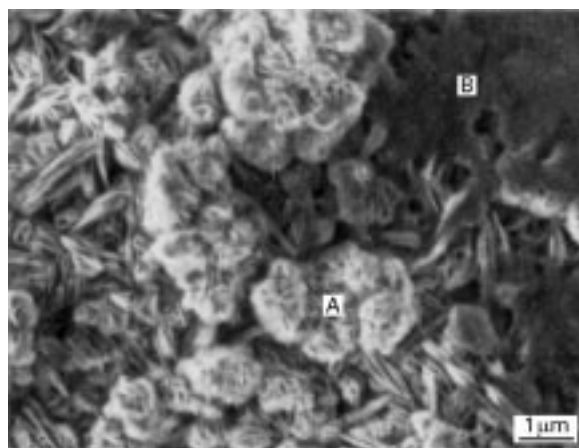


Figure 5 Silica-zinc deposit after 15 min polarization. A, zinc needles and nodules; B, amorphous silica.

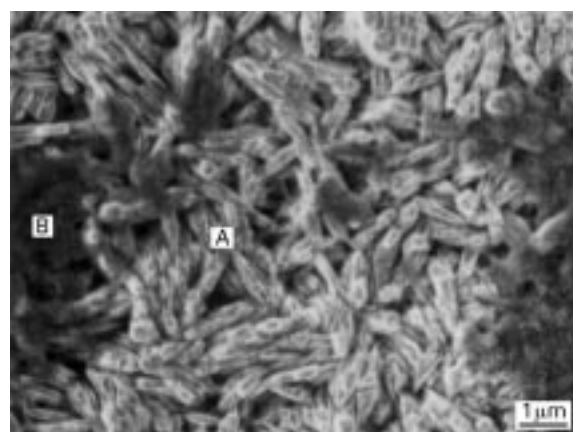


Figure 6 Silica-zinc deposit after 45 min polarization. A, zinc nodules; B, amorphous silica.

polar solvents are present. Lindquist and Stratten [23] discussed poly(ethylene imine) (PEI) adsorption on silica and showed that the particles tend to flocculate the system. They found a relation between the critical flocculation concentration and the cationic charge on the PEI. the polymer we chose here to

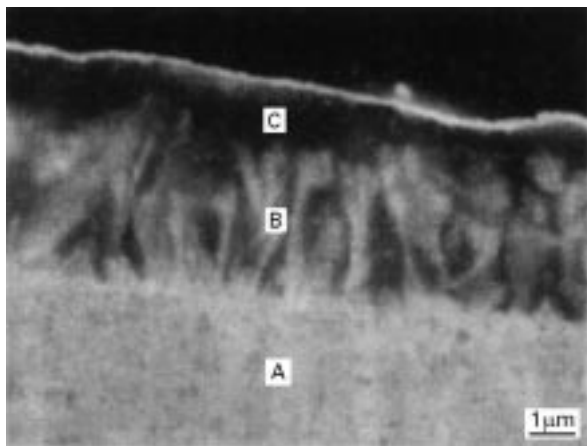


Figure 7 Profile view of a silica–zinc deposit after 45 min polarization. A, electrolytic zinc; B, area rich in zinc; C, amorphous silica.

reverse the silica surface charge is PVI. The molecule contains protonated basic amine groups in acidic media. This polymer was chosen because of its ability to complex metallic ions and because it has been reported to be stable in electrolytic cells [24]. Coating experiments were performed at pH 4, where the adsorbing molecules are close to full protonation.

Previous studies [9, 25, 26] have shown the influence of the quaternization degree, q , on the amount adsorbed on silica and therefore on the particle charge. In the present case we measure an adsorption maximum with 2% quaternized PVI (pH 7; $\Gamma = 1.3 \text{ mg m}^{-2}$). At and above 20% quaternized, PVI adsorbs less on silica (0.4 mg m^{-2}) (Fig. 8). This phenomenon is explained by intrachain and interchain repulsion forces, which are very important at high charge densities, making the polymer stretched on the surface.

Cathodic deposits can be realized at pH 4 with silica and moderately charged PVI ($2\% < q < 12\%$), at low applied voltages. At a fixed potential value (-3 V), the mass gain seems to increase regularly as a function of time (Fig. 9), and this is so for all types of PVIs. However, greater the quaternization degree, the lower is the mass gain; for 52% methylated PVI, the deposited layer is about 10 mg after 20 min, compared with 200 mg for PVI with $q = 12\%$. A possible explanation is that highly methylated molecules cannot reduce their electrical charge on the cathode, in comparison with simply protonated molecules. The deposition of a thin layer of silica particles with the former type of polymer generates therefore an accumulation of positive charges that prevent other silica particles from approaching the electrode. The lack of protons when using highly quaternized PVI is demonstrated by pH increase measured in the course of deposition (about 2 pH units increase from 4 to 6).

There is a dependence of the deposition yield on the applied voltage. Figure 10 presents deposition yields as a function of time for different applied potentials in suspensions containing silica (0.5 wt%) and 12% quaternized PVI at full surface coverage. The fact that for -5 V the mass gains are very low and irregular is due to hydrogen release on the cathode. Otherwise we

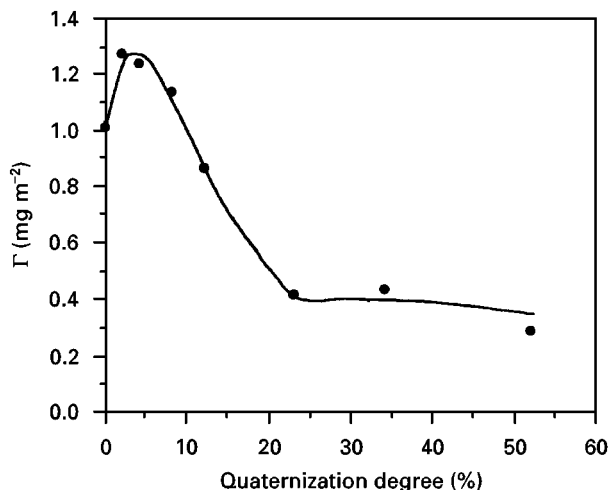


Figure 8 Adsorbed amounts in a plateau of the PVI adsorption isotherms on silica as a function of quaternization degree.

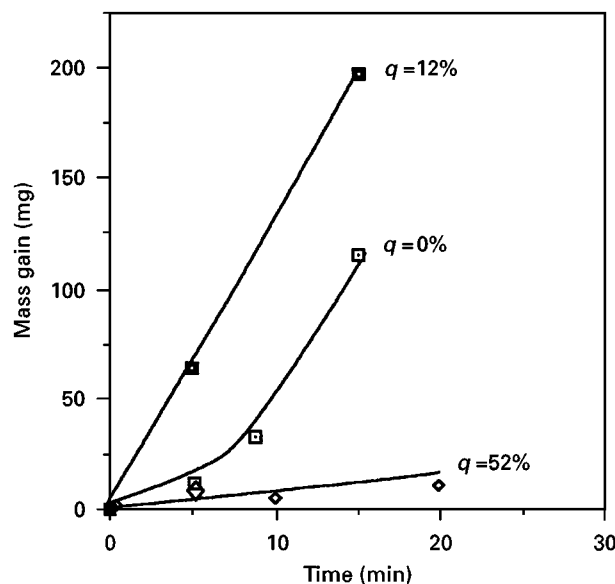


Figure 9 Silica–PVI mass gain as a function of time: influence of quaternization degree of PVI.

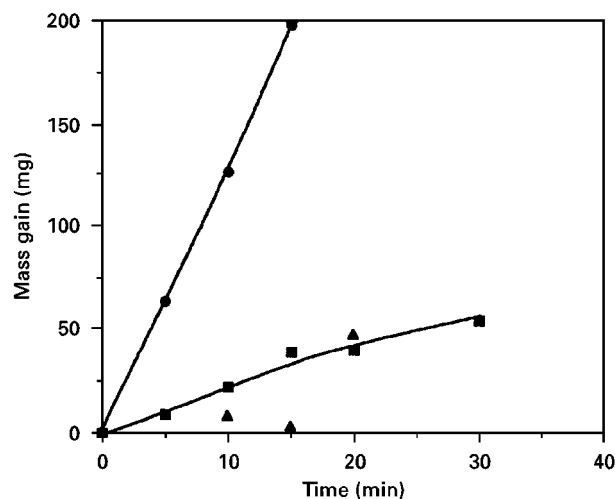


Figure 10 Silica–PVI mass gain as function of time: influence of the applied potential. (■), 2V; (●), 3V; (▲), 5V.

note that increasing the potential makes thicker coatings. At longer deposition times (and also at higher potentials) adhesion of the layer on the substrate weakens and the colour of the coating turns yellow, which is explained by the reduction of the aminated groups. At higher current density, oxidation of PVI occurs at the counter electrode [27] and the degradation of PVI leads to gas bubbling.

3.3. Silica charge control using oxide adsorption

The adsorption of an inorganic oxide on the silica surface is the third method investigated to reverse the surface charge. Positively charged silica sols of this type were developed by Alexander and Bolt [28], who defined the type of polyvalent metal oxide coating over the surface of silica particles, providing also a high sol stability. The selected sol contained 26% silica and 4% Al_2O_3 ; the positively charged particles were surrounded by chloride counterions. Similarly a titania-coated sol was made by hydrolysing an organic titanium compound in an acid-stabilized silica

sol at a pH less than 2 by heating the mixture to cause titania deposition on the particles surface [29,30]. One characteristic of these sols is that they can be dried and easily reprecipitated. The reason is that alumina-coated sols produce no soluble silica in solution and no silanol groups remain on the surface. Therefore no strong siloxane (Si-O-Si) bonds form when the sols are heated to give a powder. The stability of these positive sols has been examined by Katsanis and Matijevic [31].

As explained above, we chose cerium oxide as a positive charge promotor because it has been reported as an anticorrosion compound. It is clear that the concentration of ceria has an influence on the coverage on the charge level and on the charge sign (Fig. 11). When less than 30% of the silica surface covered with ceria, the entity still remains negative; the particles are then going to the anode. 50% coverage is required for a $-/+$ charge reversal, producing a zeta potential of 40 mV. The fact that silica and ceria have an opposite surface charge at natural pH provokes a flocculation of the system when mixing the two sols. The stabilization of the mixture is obtained by addition of PVA

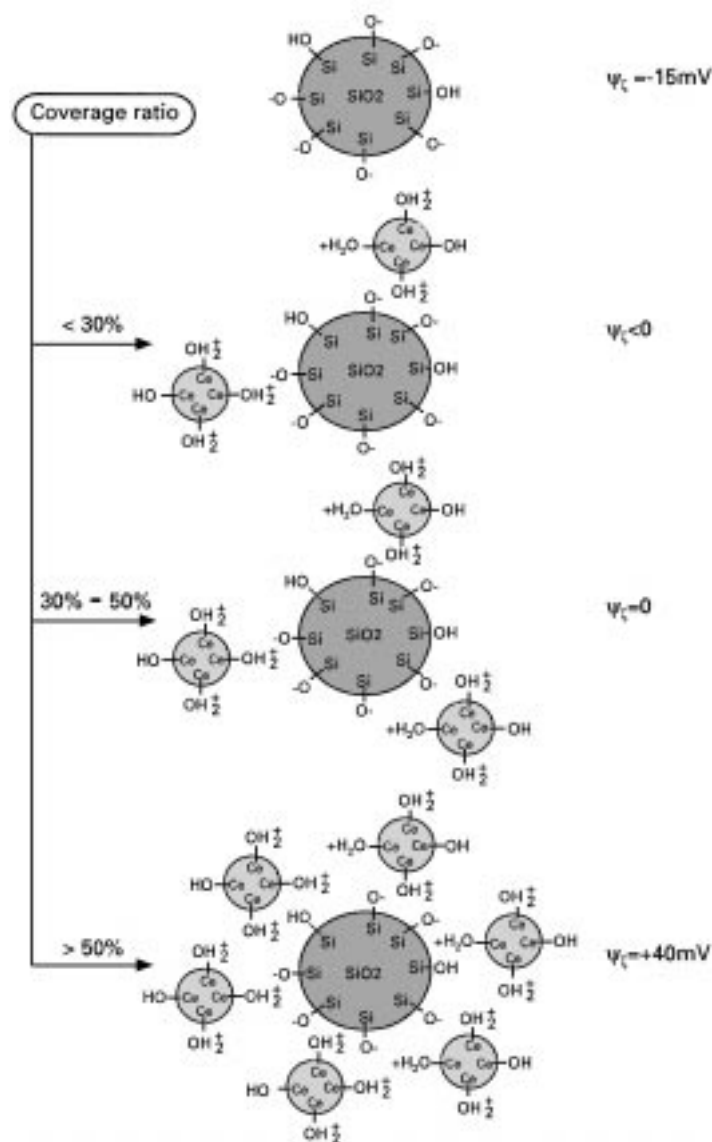


Figure 11 Influence of the CeO_2 to SiO_2 surface coverage ratio on the zeta potential.

($M_w = 49\,000\text{ g mol}^{-1}$). The polymer adsorbs on the silica surface owing to hydrogen bonding between the electron donor oxygen atoms of the polymer and the silanol groups on silica. Fig. 12 shows the adsorption isotherms of PVA on silica at different pH. When silica is strongly ionized (i.e., pH 8) the adsorption decreases in comparison with that at pH 3–4, where most of the surface is covered with unionized silanol groups.

In order to estimate the PVA influence on particle disaggregation, turbidity measurements have been done. The turbidity is defined as

$$\tau = \frac{1}{L} \ln\left(\frac{I_0}{I}\right)$$

where L is the cell thickness and I_0/I is the reciprocal of the transmission ratio. A number of measurements have been realized (Fig. 13) on different suspensions containing a PVA concentration varying from 1 to 20 g l^{-1} . The optimum PVA concentration is of about 14 g l^{-1} , giving to the system a high dispersion stability through steric repulsion forces.

Cathodic polarization have been done using a platinum counterelectrode; the electric field was set between -1 and -3 V cm^{-1} and deposition times between 2 and 20 min. In order to optimize the polarization and the deposition time, R_p measurements were made on different $\text{CeO}_2/\text{SiO}_2$ deposited layers. Table I summarizes the results obtained in polarization resistance measurements. As was mentioned before, R_p is proportional to $(i_{\text{corrosion}})^{-1}$; so the best coating produces a higher R_p value. The protective aspect of the sheet is already obtained with an electrolytic zinc and a chromate layer, since the R_p value is multiplied ten times ($164\text{ }\Omega\text{ cm}^{-2}$ to $1953\text{ }\Omega\text{ cm}^{-2}$). From this table it is clear that there is a great relation between the deposition conditions (applied potential and time deposition) and the performance of the formed layer. At fixed electric field (-2 V cm^{-1}), increasing the time deposition is a way of producing a more protective layer on the substrate; an optimum value of R_p is found for 5–10 min polarization.

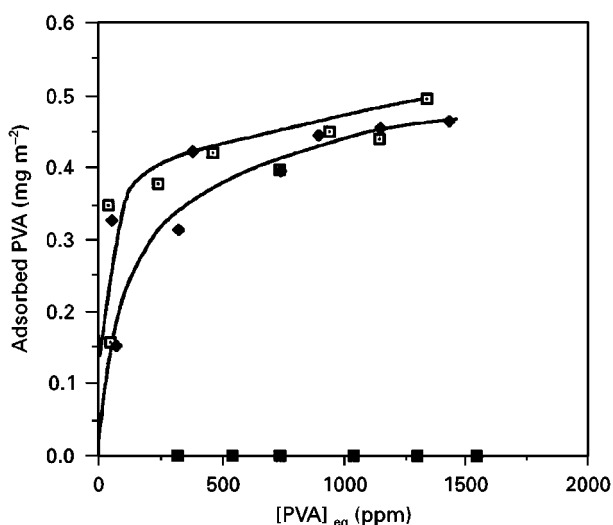


Figure 12 Adsorption isotherms of PVA ($M_w = 49\,000\text{ g mol}^{-1}$): influence of pH. (□), pH 3.5; (◇), pH 4.5; (■), pH 8.

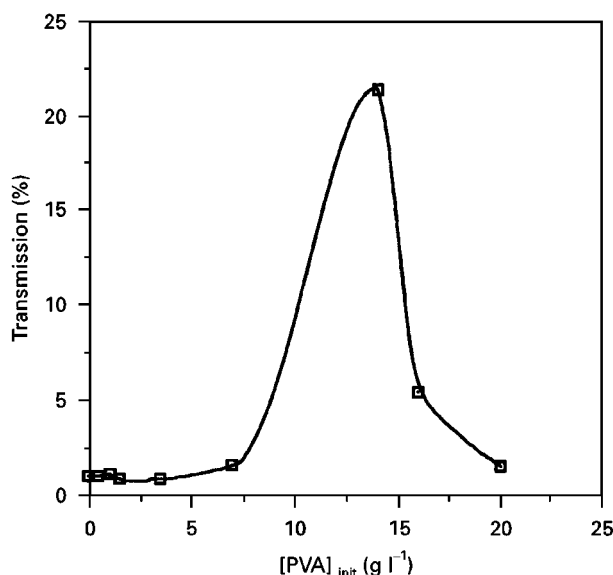


Figure 13 Influence of the PVA concentration on the suspension stability.

TABLE I Polarization resistance measurements on different substrates

		R_p ($\Omega\text{ cm}^{-2}$)
Steel		164
Zinc-coated steel		390
Chromated zinc-coated steel		1953
-2 V cm^{-1}	2 min	8013
	5 min	22321
	10 min	16622
	20 min	9328
	30 min	453
5 min	-1.5 V cm^{-1}	6649
	-2 V cm^{-1}	22321
	-2.5 V cm^{-1}	6793
	-3 V cm^{-1}	5841

Figure 14 shows a section of a deposit obtained at -2 V cm^{-1} (10 min). The deposit is quite homogeneous with a few cracks distributed over all the surface. The two chimneys on the picture are ceria-enriched areas. Besides these, the XPS analysis reveal an homogeneous distribution of silica and ceria in the layer; the thickness is about $10\text{ }\mu\text{m}$.

For longer time deposition, R_p decreases, tending to the value obtained with zinc-coated steel. At this moment the accumulation of charged particles on the surface produces hydrogen at the cathode. This gas release is responsible for the chromate layer destruction and prevents further particle deposition.

The effect of the electric field has also been investigated. At potential differences below -1.5 V cm^{-1} the electric field is too low to make the particles migrate to the cathode; no deposition occurs. On the contrary, too high potential differences (above -2.5 V cm^{-1}) create gas evolution, which induces cracks and bubbles in the deposit. The adhesion properties are significantly reduced, which explains the low R_p values.

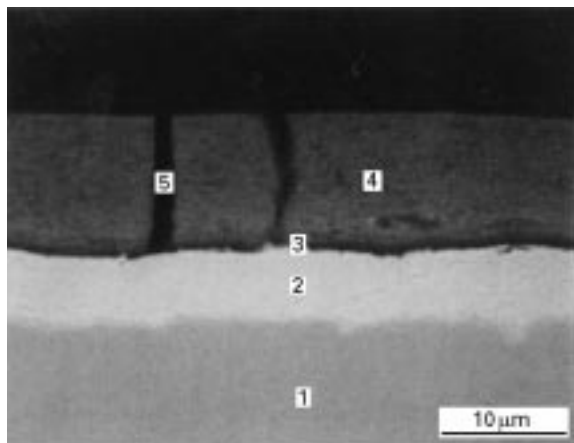


Figure 14 Profile view of a silica-ceria deposit after 10 min polarization at -2 V cm^{-1} . 1, substrate; 2, electrolytic zinc; 3, chromated layer; 4, electrophoretic deposition of silica-ceria; 5, area rich in ceria.

4. Conclusions

Cathodic deposition of silica on zinc-coated steel and on chromated zinc-coated steel is made by reversing silica surface charge. From the different processes used to charge silica positively, we can emphasise the following points.

1. The use of metallic ions such as zinc to produce this type of coating is possible only by adding PEG to the system. The cations are adsorbed on the polymer owing to polar interactions between the cations solvation water and the oxygen atoms of PEG. The layer is not very homogeneous, with most of the silica present on the surface.

2. Coatings with PVI are more uniform. A moderate polymer charge ($2\% < q < 12\%$) is a good compromise to avoid parasite electrochemical reactions, which are responsible for the PVI degradation. The applied voltage should not be above -3 V to avoid hydrogen release.

3. With cerium oxide, the phenomenon of flocculation, which is generated by opposite surface charges of ceria and silica, is solved by the use of PVA (14 g l^{-1}) in the bath formulation. This polymer allows steric stabilization of the system. At moderate electric field (-2 V cm^{-1}), the protective effect is proved by polarization resistance measurements. For a time deposition of 5–10 min, the R_p values are more than hundred times higher than with untreated steel substrates. Latex is also needed to avoid crack formation during drying.

Acknowledgements

This work was partly supported by Fransk-Norsk Stiftelse (French-Norwegian Foundation for Research

and Industrial Development) and by the Conseil Général de Franche-Comté, France.

References

1. P. SARKAR and P. S. NICHOLSON, *J. Amer. Ceram. Soc.* **79** (1996) 1987.
2. A. FOISSY, Thesis, Besançon (1975).
3. A. FOISSY and G. ROBERT, *Amer. Ceram. Soc. Bull.* **61** (1982) 251.
4. P. SARKAR, X. HAUNG and P. S. NICHOLSON, *J. Amer. Ceram. Soc.* **75** (1992) 2907.
5. G. HEIN, H. MÜLLER, H. PIEL, L. PONTO, U. BECKS, U. KLEIN and M. PEININGER, *J. Appl. Phys.* **66** (1989) 5940.
6. K. S. CHANG, *J. Colloid Interface Sci.* **165** (1994) 169.
7. A. KOZAWA, *J. Inorg. Nucl. Chem.* **21** (1961) 315.
8. R. K. ILLER, *J. Colloid Interface Sci.* **37** (1971) 364.
9. M. R. BÖHMER, W. H. A. HEESTERBEEK, A. DERATANI and E. RENARD, *Colloids Surf. A* **99** (1995) 53.
10. M. NABAVI, O. SPALLA and B. CABANE, *J. Colloid Interface Sci.* **160** (1993) 459.
11. B. PÖPPING, Thesis Paris VI (1993).
12. C. J. G. VAR DER GRIFT, A. MILDER and J. W. GEUS, *Colloid Surf. A* (1991) 223.
13. O. DE SANCTIS, *J. Non-Cryst. Solids* **120** (1990) 338.
14. M. ATIK, P. DE LIMA NETO, M. A. AEGERTER and L. A. AVACA, *J. Appl. Electrochem.* **25** (1995) 142.
15. H. C. HAMAKER and E. J. W. VERWEY, *Trans. Faraday Soc.* **36** (1940) 180.
16. E. E. BIBIK, I. S. LAVROV and O. M. MERKUSHEV, *Kolloidnyi Z.* **30** (1968) 494.
17. D. D. MAC DONALD, *J. Electrochem. Soc.* **125** (1978) 1443.
18. M. STERN and A. L. GEARY, *J. ibid.* **104** (1956) 56.
19. S. AHRLAND and I. GRENTHE, *Acta Chem. Scand.* **14** (1960) 1059.
20. R. O. JAMES and T. W. HEALY, *J. Colloid Interface Sci.* **40** (1972) 65.
21. J. PERSELLO and A. FOISSY, in "Surface chemistry of silicas", edited by P. J. Legrand (Wiley, New York, 1998) 365.
22. A. TAKAHASHI, Y. MIYOSHI and T. HADA, *J. Electrochem. Soc.* **141** (1994) 954.
23. G. M. LINDQUIST and R. A. STRATTEN, *J. Colloid Interface Sci.* **55** (1976) 45.
24. N. DESBOIS, Thesis, Besançon (1992).
25. B. CABOT, A. DERATANI and A. FOISSY, *Colloids & Surfaces A*, **139** (1998) 287.
26. B. CABOT, Thesis, Besançon (1997).
27. K. KHAM, A. DERATANI, B. SEBILLE, J. GAL and L. T. YU, *New J. Chem.* **16** (1992) 505.
28. G. B. ALEXANDER and G. H. BOLT, US Patent 3 007 878 (Du Pont) (1961).
29. M. MINDICK and A. C. THOMPSON, US Patent 3 244 639 (Nalco Chemical Co.) (1966).
30. *Idem*. US Patent 3 252 917 (Nalco Chemical Co.) (1966).
31. E. P. KATSANIS and E. MATIJEVIC, in Proceedings of the 49th National Colloid Symposium, Postdam, NY, (1975).

Received 29 April 1997

and accepted 11 May 1998